Available online at www.sciencedirect.com
ScienceDirect
Ceramics International 37 (2011) 3117–3121
CERAMICS INTERNATIONAL
www.elsevier.com/locate/ceramint

Formation, densification, and selected mechanical properties of hot pressed Al_4SiC_4, Al_4SiC_4 with 30 vol.% WC, and Al_4SiC_4 with 30 vol.% TiC

Osama Gaballa [a,b,c,*], Bruce Cook [b], Alan Russell [a,b]

[a] Department of Materials Science and Engineering, Iowa State University, Ames, IA 50011, USA
[b] Ames Laboratory Division of Materials Science and Engineering, Iowa State University, Ames, IA 50011, USA
[c] Central Metallurgical Research and Development Institute, Helwan, Cairo, Egypt

Received 30 March 2011; received in revised form 13 May 2011; accepted 13 May 2011
Available online 24 May 2011

Abstract

Powders of Al_4C_3 and SiC were combined by high-energy milling to produce Al_4SiC_4, Al_4SiC_4 + 30 vol.% TiC, and Al_4SiC_4 + 30 vol.% WC. Five different temperatures were used to hot press the constituents. XRD, SEM, relative density, and hardness measurements showed that formation of single-phase Al_4SiC_4 occurred at 1450 °C and full densification (99%) was achieved at 1500 °C. Both of these temperatures are lower than previously reported. Adding TiC and WC increases hardness, while WC improves densification (99.5%).
Published by Elsevier Ltd and Techna Group S.r.l.

Keywords: A. Hot pressing; D. Carbides; Aluminum silicon carbide; Densification

1. Introduction

Al_4SiC_4 is a low density (3.03 g/cm^3), high melting temperature (>2000 °C) compound, characterized by superior oxidation resistance, and high compressive strength [1–5]. These desirable properties motivated several investigators to determine the material's high-temperature strength, thermal conductivity, temperature dependence of linear thermal expansion coefficient, heat capacity from 5.26 to 1047 K, temperature dependence of electrical resistivity, and equation of state [3,6–9]. Additional work has been performed on the synthesis, densification, microstructure, and mechanical properties of Al_4SiC_4 [5,10–16]. Some work has also been performed on the effects of C, AlN, and SiC additions to Al_4SiC_4 [17,18].

In all earlier work reported on Al_4SiC_4, the sintering temperature was above 1600 °C, and many of these trials involved other phases mixed with the Al_4SiC_4. In this study, we attempted to obtain high-density Al_4SiC_4 at lower sintering temperatures by hot pressing and by adding two different materials, WC and TiC, to the Al_4SiC_4.

2. Experimental

2.1. Preparation of the starting powders

The Al_4SiC_4 starting powder for this study was prepared by mixing high-purity Al_4C_3 and SiC (99.8% purity) powders in a He-atmosphere. A Spex-8000 mixer/mill was used to comminute the powders in sealed, hardened steel vials with chrome steel milling media. The constituents were milled for 6 h, a milling time found to be suitable in earlier studies on processing TiB_2–ZrB_2 and TiB_2 [19,20]. For some samples, the mechanically alloyed Al_4SiC_4 powder was then mixed with 30 vol.% TiC or 30 vol.% WC and milled for an additional 30 min. The second-phase additions were 99.5% pure, 1 μm average size for WC and 2 μm for TiC. All powder handling occurred in a He-atmosphere glove box to minimize oxygen contamination.

2.2. Consolidation

Powder consolidation was performed in a 75-ton Centorr hot press using graphite dies under a flowing argon atmosphere. All samples were pressed for 60 min at a pressure of 106 MPa. The dies were lined with boron nitride and graphite sheet as lubricants. Al_4SiC_4 samples were pressed at five different temperatures, 1200 °C, 1300 °C, 1400 °C, 1450 °C, and

* Corresponding author at: Department of Materials Science and Engineering, Iowa State University, Ames, IA 50011, USA.
E-mail address: ogaballa@iastate.edu (O. Gaballa).

0272-8842/$36.00. Published by Elsevier Ltd and Techna Group S.r.l.
doi:10.1016/j.ceramint.2011.05.050

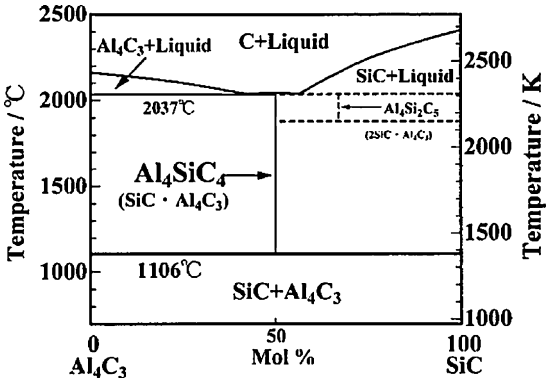

Fig. 1. The phase diagram for SiC–Al_4C_3 system [14].

1500 °C. Al_4SiC_4 + 30% WC and Al_4SiC_4 + 30% TiC specimens were pressed only at 1500 °C (Fig. 1).

2.3. Evaluation

XRD was used to identify the formation of Al_4SiC_4 phase in all specimens. The hot-pressed microstructures were analyzed by SEM and EDS. Density was determined by the Archimedes displacement method; the sintered specimen was weighed in air, and the sample was then lowered into water to measure its weight in water. Then the relative density of the sintered materials was calculated according to the following formula: Relative density (D) % = ρ_s/ρ_t where ρ_s is the sintered density (actual density), and ρ_t the theoretical density respectively. Hardness was measured at a load of 2000 g by Vickers microindentation with a Wilson-Tukon 2100B microhardness tester equipped with CCD image enhancement capability. The hardness values of the investigated materials were measured as the average of ten readings along the cross section surface of polished specimens.

3. Results and discussion

3.1. Formation, densification, and XRD analysis of the samples

Al_4SiC_4 can be obtained from the following reaction [21]. SiC + Al_4C_3 → Al_4SiC_4 The standard Gibbs energy of formation for this reaction changes from positive to negative at 1106 °C. Therefore, formation of the ternary compound is favored at temperatures above 1106 °C, as can be seen from the phase diagram for SiC–Al_4C_3 system. Actually, the detection of Al_4SiC_4 starts at 1200 °C so this temperature was used as the first in a series of sintering temperatures [14,2].

The degree of densification achieved during hot-pressing of powders relates to several variables: powder particle size, powder handling atmosphere, milling conditions, sintering temperature, and hot pressing pressure. For example, a mixture of particle sizes can improve the fill ratio of a pressed compact. Also, milling under an inert atmosphere produces surfaces nearly free of oxides, which have high activity and are more readily sintered. High pressure during sintering generally increases densification [22–24].

Fig. 2 shows the XRD patterns of the Al_4SiC_4 sintered samples hot pressed for 1 h at five different temperatures (1200 °C, 1300 °C, 1400 °C, 1450 °C, and 1500 °C). Fig. 3 shows the XRD patterns for Al_4SiC_4, Al_4SiC_4 + 30% TiC, and Al_4SiC_4 + 30% WC samples sintered at 1500 °C for 1 h.

As shown in Fig. 2, the XRD patterns of the powders sintered at 1200 °C and 1300 °C clearly show the presence of four phases, SiC, Al_4C_3, the Al_4SiC_4 reaction product plus Fe from milling wear debris. Prior work on related materials indicates that the Fe content may be less than 1.5% [25], the intensity of the iron peak is strong due to the higher atomic number of the iron compared to the atomic number of the Al_4SiC_4. At these two temperatures, the two starting powder phases are dominant. At 1400 °C, however, the Al_4SiC_4 phase dominates, and at 1450 °C, and 1500 °C Al_4SiC_4 is the only non-ferrous crystalline phase detected. Taken together, these patterns show that Al_4C_3 and SiC powders can be fully reacted to Al_4SiC_4 by milling 6 h and hot pressing for 1 h at 106 MPa and 1450 °C.

The XRD patterns show hexagonal crystal structures for two detected phases of Al_4SiC_4 and WC and a cubic crystal structure for the TiC. As shown in Fig. 3 middle and 3 top, the intensities of Al_4SiC_4 peaks are low relative to those of TiC and WC, presumably due to the large differences in atomic weights of the elements in these three phases. Also, fewer peaks are observed in Fig. 3 middle than in Fig. 3 bottom and 3 top. This could be explained by the negative correlation between the crystal symmetry and the number of peaks. In support of this explanation, the cubic structure, which has the highest symmetry, was found to give rise to the minimum number of peaks [26].

These results indicate that hot pressing of Al_4C_3 and SiC with TiC or WC milled powders for 1 h under a pressure of 106 MPa at 1500 °C is adequate to produce two-phase Al_4SiC_4 + TiC or Al_4SiC_4 + WC with reasonably good phase purity.

3.2. Microstructure

Most of the phases were found to be smaller than 1 μm, except for WC, where abnormal grain growth was observed (Fig. 4c). This grain growth in the presence of carbon has been

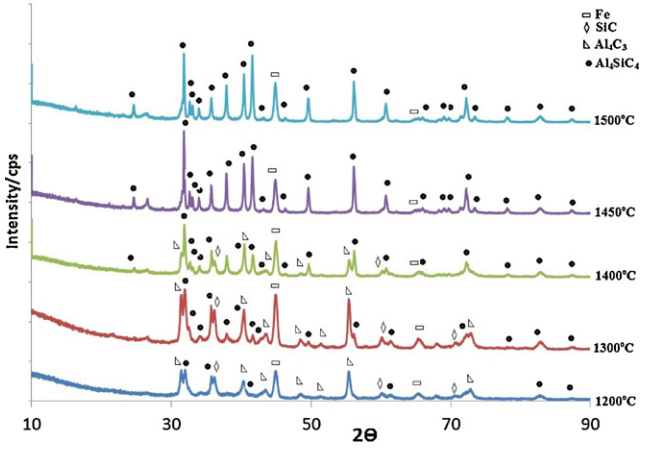

Fig. 2. XRD patterns of the various hot-pressed powders of Al_4SiC_4 at 1200 °C, 1300 °C, 1400 °C, 1450 °C, and 1500 °C for 1 h in flowing Ar. Fe is present in these samples from wear debris during milling.

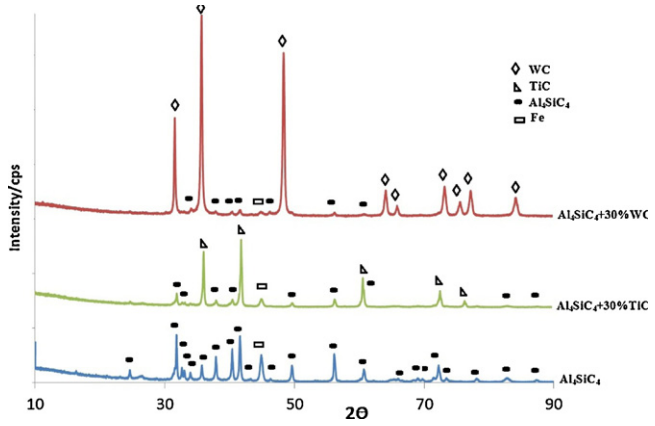

Fig. 3. XRD patterns of Al_4SiC_4, Al_4SiC_4 + 30%, and Al_4SiC_4 + 30% TiC hot pressed at 1500 °C for 1 h in flowing Ar.

noted before but is not totally understood. This may be explained by the presence of carbon, which could lower the activation energy of two-dimensional nucleation on singular grain boundary surfaces of WC [27]. In contrast, the Al_4SiC_4 + 30% TiC showed no abnormal grain growth, which is consistent with previous observations that TiC can prevent grain growth during sintering [23,24].

3.3. Mechanical properties

3.3.1. Relative density

We found that the relative densities of hot-pressed Al_4SiC_4 were significantly increased as temperature increased and reached nearly full densification at 1500 °C (Fig. 5). The high relative density percentages are thought to result mainly from rearrangement of grains, which results in closer packing. Also, the closer packing of grains may be partly promoted by hot pressing [28].

Table 1 shows the 1500 °C densification values for the three compositions examined in this study. It can be seen that the Al_4SiC_4 achieves nearly full densification (98.8%), while addition of WC gave rise to higher densification (99.5%), and addition of TiC resulted in reduced densification (98%). The lower densification of Al_4SiC_4 + TiC was expected due to the higher consolidation temperature required for TiC [29]. A similar trend for Al_4SiC_4 + WC was expected, but the results of the relative densities show higher densification. It is unclear why this occurred, but it may be due to the carbon content in the Al_4SiC_4 + WC, where the presence of sufficient carbon can help the densification of WC as previously stated. The presence of sufficient carbon is consistent with the fact that all the experiments were performed in a controlled atmosphere in order to keep the oxygen content as low as possible and subsequently prevent decarburization due to reduction of surface oxide. In support of this explanation, Oscroft et al. [28] reported that the presence of oxygen in the chamber consumes carbon and consequently reduces the carbon content. The XRD

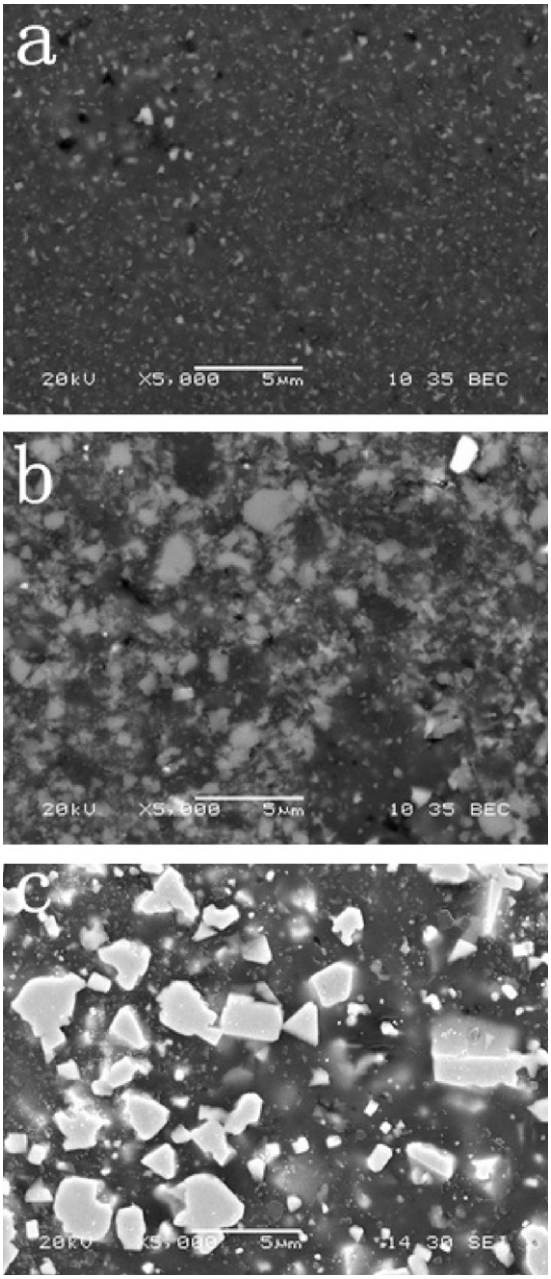

Fig. 4. Back-scattered SEM micrographs of (a) Al_4SiC_4, and (b) Al_4SiC_4 + -TiC, and secondary electron micrograph of (c) Al_4SiC_4 + WC.

Table 1
Comparison of some properties of carbides. *Indicates results from current study.

	Ti_3SiC_2 [3]	Ti_3AlC_2 [3]	Al_4SiC_4*	Al_4SiC_4 + 30% WC*	Al_4SiC_4 + 30% TiC*
Theoretical density (g/cm^3)	4.53	4.21	3.03	6.83	3.6
Relative density (%)	99	99	98.8	99.5	98
Vickers hardness (GPa)	4	3.5	12.7	14.6	15.5

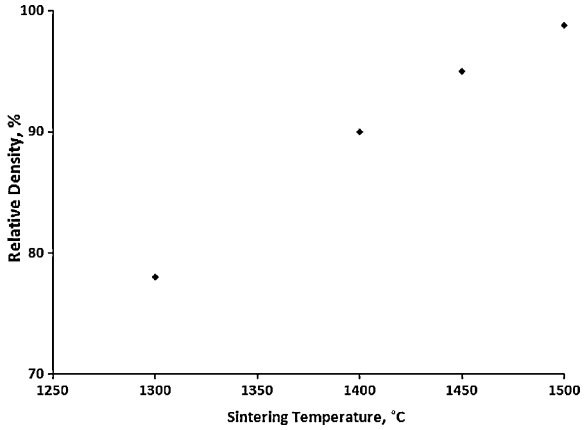

Fig. 5. Effect of sintering temperature on the relative density of hot-pressed Al_4SiC_4.

results confirmed the absence of W_2C, which supports the idea of preventing decarburization [30]. Finally, the presence of sufficient carbon content leads to abnormal grain growth, which can be supported by the SEM micrographs [27,30–32].

Hot pressing TiC and WC to high density at 1500 °C is notable, because this temperature corresponds to only 47% and 52% of the absolute melting temperatures of TiC and WC, respectively.

3.3.2. Hardness

As shown in Fig. 6, the hardness values of hot-pressed Al_4SiC_4 increase with increasing sintering temperatures. In Table 1 the maximum Vickers hardness for Al_4SiC_4 of 12.73 GPa agrees well with the value reported previously [16]. The 14.63 GPa hardness of Al_4SiC_4 + 30% WC and the 15.5 GPa hardness of Al_4SiC_4 + 30% TiC were expected due to the higher hardness values of WC and TiC.

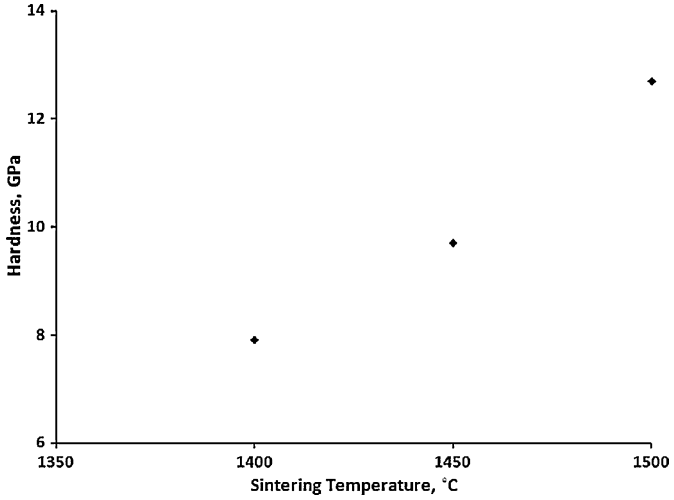

Fig. 6. Effect of sintering temperature on the hardness of hot-pressed Al_4SiC_4. Note that there are no values below 1400 °C because the samples were too porous to be measured.

Table 1 compares theoretical density, relative density, and hardness values of Al_4SiC_4, Al_4SiC_4 + 30% WC, and Al_4SiC_4 + 30% TiC to the values for two other ternary carbides, Ti_3SiC_2 and Ti_3AlC_2. The hardness values of Ti_3SiC_2 and Ti_3AlC_2 are much lower than those of the materials used in this study. These lower values can be attributed to the planar Si layers linked together by TiC octahedra, forming a highly deformable basal slip plane [33]. However, in the crystal structure of Al_4SiC_4, such a weak connective layer may not exist [1].

4. Conclusions

1. Single-phase Al_4SiC_4 was produced at 1450 °C, which is a lower temperature than has been previously reported.
2. Full densification of Al_4SiC_4 occurred at 1500 °C
3. As expected, the Al_4SiC_4 specimens containing 30% TiC and WC had higher hardness than single-phase Al_4SiC_4.
4. Adding WC to Al_4SiC_4 increased densification to 99.5%.

Acknowledgements

Work at the Ames Laboratory was supported by the U.S. Department of Energy, Division of Materials Science & Engineering under contract DE-AC02–07CH11358. One of the authors (OG) wishes to acknowledge support from the Egyptian Ministry of Higher Education and Scientific Research.

References

[1] Z. Inoue, Y. Inomata, H. Tanaka, H. Kawabata, X-ray crystallographic data on aluminum silicon carbide, α-Al_4SiC_4 and $Al_4Si_2C_5$, Journal of Materials Science 15 (3) (1980) 575–580.
[2] S.U.H. Yokokawa, M. Fujita, M. Dokiya, Phase relation associated with the aluminum blast furnace: aluminum oxycarbide melts and Al–C–X (X = Fe, Si) liquid alloy, Metallurgical Transactions B 18B (1987) 433–444.
[3] G. Wen, X. Huang, Increased high temperature strength and oxidation resistance of Al_4SiC_4 ceramics, Journal of the European Ceramic Society 26 (7) (2006) 1281–1286.
[4] S.M. Koji Inoue, A. Yamaguchi, Oxidation behavior of Al_4SiC_4-SiC sintered bodies, Journal of the Ceramic Society of Japan 111 (1290) (2003) 126–132.
[5] X. Huang, G. Wen, X. Cheng, B. Zhang, Oxidation behavior of Al_4SiC_4 ceramic up to 1700 °C, Corrosion Science 49 (5) (2007) 2059–2070.
[6] V. Solozhenko, O. Kurakevych, Equation of state of aluminum silicon carbide [alpha]-Al_4SiC_4, Solid State Communications 135 (1–2) (2005) 87–89.
[7] S.M. Koji Inoue, A. Yamaguchi, Thermal conductivity and temperature dependence of linear thermal expansion coefficient of Al_4SiC_4 sintered bodies prepared by pulse electronic current sintering, Journal of the Ceramic Society of Japan 111 (1293) (2003) 348–351.
[8] R. Beyer, E. Johnson, Heat capacity of aluminum silicon carbide (Al_4SiC_4) from 5.26 to 1047 K, The Journal of Chemical Thermodynamics 16 (11) (1984) 1025–1029.
[9] S.M. Koji Inoue, A. Yamaguchi, Temperature dependence of electrical resistivity of the Al_4SiC_4 sintered bodies prepared by pulse electronic current sintering, Journal of the Ceramic Society of Japan 111 (1292) (2003) 267–270.
[10] J. Lee, S. Lee, T. Nishimura, H. Tanaka, Synthesis of mono-phase, hexagonal plate-like Al_4SiC_4 powder via a carbothermal reduction process, Journal of the Ceramic Society of Japan 116 (1354) (2008) 717–721.

[11] H Jian-feng, Z. Xie-rong, L. He-jun, X. Xin-bo, H. Min, Al_2O_3-mullite-SiC-Al_4SiC_4 multi-composition coating for carbon/carbon composites, Materials Letters 58 (21) (2004) 2627–2630.
[12] O. Yamamoto, M. Ohtani, T. Sasamoto, Preparation and oxidation of Al_4SiC_4, Journal of Materials Research 17 (4) (2002) 774–778.
[13] J. Zhao, W. Lin, A. Yamaguchi, J. Ommyoji, J. Sun, Synthesis of Al_4SiC_4 from alumina, silica and graphite, Journal of the Ceramic Society of Japan 115 (1347) (2007) 761–766.
[14] K. Inoue, A. Yamaguchi, Synthesis of Al_4SiC_4, Journal of the American Ceramic Society 86 (6) (2003) 1028–1030.
[15] O. Yamamoto, Effect of triethanolamine on low-temperature preparation of aluminum silicon carbide, Solid State Sciences 5 (2) (2003) 277–279.
[16] K. Itatani, F. Takahashi, M. Aizawa, I. Okada, I. Davies, H. Suemasu, A. Nozue, Densification and microstructural developments during the sintering of aluminium silicon carbide, Journal of Materials Science 37 (2) (2002) 335–342.
[17] S.M. Koji Inoue, A. Yamaguchi, Journal of the Ceramic Society of Japan 111 (1295) (2003) 466–470.
[18] J.O. Motonari Fujita, A. Yamaguchi, Influence of carrbon on sintering of the Al–Si–C–N system composite, Journal of the Ceramic Society of Japan 115 (4) (2007) 272–277.
[19] J. Peters, B. Cook, J. Harringa, A. Russell, Microstructure and wear resistance of low temperature hot pressed TiB_2, Wear 266 (11–12) (2009) 1171–1177.
[20] J. Peters, B. Cook, J. Harringa, A. Russell, Erosion resistance of TiB_2–ZrB_2 composites, Wear 267 (1–4) (2009) 136–143.
[21] S. Kang, D. Kim, Synthesis of nano-titanium diboride powders by carbothermal reduction, Journal of the European Ceramic Society 27 (2–3) (2007) 715–718.
[22] R. Königshofer, S. Fürnsinn, P. Steinkellner, W. Lengauer, R. Haas, K. Rabitsch, M. Scheerer, Solid-state properties of hot-pressed TiB_2 ceramics, International Journal of Refractory Metals and Hard Materials 23 (4–6) (2005) 350–357.
[23] M. Gu, C. Huang, B. Zou, B. Liu, Effect of (Ni, Mo) and TiN on the microstructure and mechanical properties of TiB_2 ceramic tool materials, Materials Science and Engineering: A 433 (1–2) (2006) 39–44.
[24] J. Kim, H. Chung, S. Lee, K. Oh, J. Shim, Y. Cho, Mechanochemical synthesis of TiN/TiB_2/Ti-silicide nanocomposite powders and their thermal stability, Intermetallics 15 (2) (2007) 206–210.
[25] S. Shvab, P. Kislyi, Some properties of tantalum carbide powder produced by synthesis from the elements, Powder Metallurgy and Metal Ceramics 13 (5) (1974) 368–370.
[26] M. De Graef, M. McHenry, Structure of Materials: An Introduction to Crystallography, Diffraction and Symmetry, Cambridge University Press, 2007
[27] S Cha, S. Hong, B. Kim, Spark plasma sintering behavior of nanocrystalline WC-10Co cemented carbide powders, Materials Science and Engineering: A 351 (1–2) (2003) 31–38.
[28] R. Oscroft, D. Thompson, Influence of oxygen on the formation of aluminum silicon carbide, Journal of the American Ceramic Society 75 (1) (1992) 224–226.
[29] L.K.R. Chaim, S. Kalabukhov, Densification of nanocrystalline tic ceramics by spark plasma sintering, International Journal of Applied Ceramic Technology, in press.
[30] K. Tsai, The effect of consolidation parameters on the mechanical properties of binderless tungsten carbide, International Journal of Refractory Metals and Hard Materials 29 (2011) 188–201.
[31] T. Li, Q. Li, J. Fuh, P. Yu, C. Wu, Effects of lower cobalt binder concentrations in sintering of tungsten carbide, Materials Science and Engineering: A 430 (1–2) (2006) 113–119.
[32] K. Tsai, C. Hsieh, H. Lu, Sintering of binderless tungsten carbide, Ceramics International 36 (2) (2010) 689–692.
[33] J. Viala, N. Peillon, F. Bosselet, J. Bouix, Phase equilibria at 1000 °C in the AlCSiTi quaternary system: an experimental approach, Materials Science and Engineering: A 229 (1–2) (1997) 95–113.